PROCEEDINGS OF SCIENCE

# Hadronic light-by-light contribution to $(g-2)_\mu$ from lattice QCD: a complete calculation

**En-Hung Chao,**[a,*] **Renwick J. Hudspith,**[a] **Antoine Gérardin,**[b] **Jeremy R. Green,**[c,1] **Harvey B. Meyer**[a,d,e] **and Konstantin Ottnad**[a]

[a] *PRISMA$^+$ Cluster of Excellence & Institut für Kernphysik, Johannes Gutenberg-Universität Mainz, D-55099 Mainz, Germany*

[b] *Aix Marseille Univ, Université de Toulon, CNRS, CPT, Marseille, France*

[c] *Theoretical Physics Department, CERN, 1211 Geneva 23, Switzerland*

[d] *Helmholtz Institut Mainz, Staudingerweg 18, D-55128 Mainz, Germany*

[e] *GSI Helmholtzzentrum für Schwerionenforschung, Darmstadt, Germany*

*E-mail:* enchao@uni-mainz.de

The tension between the theoretical prediction and the experimental result of the anomalous magnetic moment of the muon, $a_\mu \equiv (g-2)_\mu/2$, is one of the long-standing puzzles of modern particle physics. After the update of the Fermilab E989 experiment in April 2021, the discrepancy between theory and experiment lies at the 4.2-sigma level. Further possible reduction of the error on the theory side relies solely on the control over hadronic processes. With recent developments, it has become possible for lattice QCD to provide competitive predictions on some of the most important hadronic contributions to $a_\mu$. In this talk, the Mainz determination of the hadronic light-by-light (hlbl) contribution to $a_\mu$ computed with $N_f = 2+1$ lattice ensembles will be presented. Although at subleading order in $\alpha_{\rm QED}$, $a_\mu^{\rm hlbl}$ was not sufficiently precisely determined in the past and represented a non-negligible source of uncertainty for the total error budget of $a_\mu$. With our continuum and infinite-volume QED setup, we obtain a value of $a_\mu^{\rm hlbl} = 106.8(15.9)\times 10^{-11}$ after an infinite-volume, continuum and chiral extrapolation, with estimates for the contributions of all five Wick-contraction topologies.

MITP-21-050

*The 38th International Symposium on Lattice Field Theory, LATTICE2021 26th-30th July, 2021 Zoom/Gather@Massachusetts Institute of Technology*

[1] Present address: School of Mathematics and Hamilton Mathematics Institute, Trinity College, Dublin 2, Ireland

[*] Speaker





PoS(LATTICE2021)209

## 1. Introduction

The anomalous magnetic moment of the muon ($a_\mu$) offers a unique opportunity to probe the validity of the Standard Model of particle physics thanks to the accuracy of its measured value. After the announcement of the first Fermilab E989 result in April 2021 [1], $a_\mu$ is known to a precision of 0.35 ppm, upon performing an average with the measurement of the completed E821 experiment at Brookhaven [2].

The muon, being much heavier than the electron, is more sensitive to hadronic (QCD) physics. Due to the non-perturbative nature of QCD at low energies, the uncertainty of the current theory prediction is dominated by the hadronic contributions to $a_\mu$. Contrary to the dominant hadronic contribution, the Hadronic Vacuum Polarization, which is of order $\mathrm{O}(\alpha_{\mathrm{QED}}^2)$ in the perturbative QED-coupling counting, the HLbL enters at $\mathrm{O}(\alpha_{\mathrm{QED}}^3)$ and is a sub-leading contribution. Still, the rather large relative error of the HLbL contribution to $a_\mu$ ($a_\mu^{\mathrm{hlbl}}$) makes a statistically-precise determination of this quantity necessary. It is thought that $a_\mu^{\mathrm{hlbl}}$ needs to be known at the 10%-level to allow the theory precision to be comparable to the experimental one.

As of the current theory consensus, dispersive methods gave the more precise estimate for $a_\mu^{\mathrm{hlbl}}$ (see Ref. [3] and references therein). In the past few years, lattice determinations of $a_\mu^{\mathrm{hlbl}}$ have become competitive with dispersive approaches. The first complete lattice determination of $a_\mu^{\mathrm{hlbl}}$ at the physical point has been published by the RBC/UKQCD collaboration [4] in a lattice QED+QCD setup. In this talk, I will present the work of the Mainz group on the determination of the $a_\mu^{\mathrm{hlbl}}$ at the physical point [5], which is based on a continuum and infinite-volume QED + lattice QCD setup.

## 2. Position space approach

To compute $a_\mu^{\mathrm{hlbl}}$, we adopt a setup which treats the QED contribution in the continuum and infinite-volume and the QCD part on the lattice [6]. More precisely, our master formula reads

$$a_\mu^{\mathrm{hlbl}} = \frac{m_\mu e^6}{3} \int_{x,y} \mathcal{L}_{[\rho,\sigma];\mu\nu\lambda}(x,y) i\hat{\Pi}_{\rho;\mu\nu\lambda\sigma}(x,y)\,, \tag{1}$$

where $\mathcal{L}_{[\rho,\sigma];\mu\nu\lambda}$ is a QED kernel,

$$i\hat{\Pi}_{\rho;\mu\nu\lambda\sigma} = -\int_z z_\rho \tilde{\Pi}_{\mu\nu\sigma\lambda}\,, \quad \tilde{\Pi}_{\mu\nu\sigma\lambda}(x,y,z) \equiv \left\langle j_\mu(x) j_\nu(y) j_\sigma(z) j_\lambda(0)\right\rangle_{\mathrm{QCD}}\,, \tag{2}$$

and $j_\mu$ is the hadronic component of electromagnetic current, which in $N_f = 2+1$ quark flavors equals

$$j_\mu(x) = \frac{2}{3}(\bar{u}\gamma_\mu u)(x) - \frac{1}{3}(\bar{d}\gamma_\mu d)(x) - \frac{1}{3}(\bar{s}\gamma_\mu s)(x)\,. \tag{3}$$

With our approach, the hadronic 4-point function $\tilde{\Pi}_{\mu\nu\sigma\lambda}$ is evaluated on the lattice in a pure QCD background.

The QED kernel requires several multidimensional integrals and is computed using the Gegenbauer polynomial expansion technique [7]. In the construction, we explicitly restore the O(4)-symmetry of the QED kernel. This allows us to write, according to the Lorentz-covariance structure:

$$a_\mu^{\mathrm{hlbl}} = \lim_{|y|_{\max}\to\infty} a_\mu^{\mathrm{hlbl}}(|y|_{\max})\,, \quad a_\mu^{\mathrm{hlbl}}(|y|_{\max}) \equiv \int_0^{|y|_{\max}} d|y| f(|y|)\,, \tag{4}$$

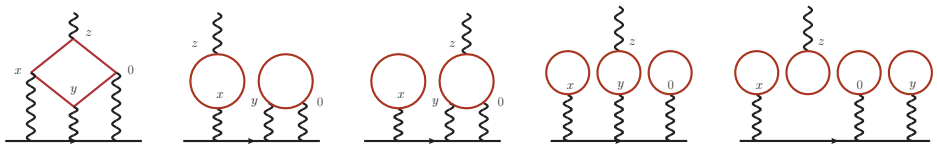


**Figure 1:** The 5 different contraction topologies appearing in the computation of the 4-point function $\tilde{\Pi}$ on the lattice. The quark propagators represented by solid red lines are computed on an ensemble of non-perturbative SU(3)-gauge fields.

where the $x$- and $z$-integrals are computed within $f(|y|)$ (as discrete sums within a lattice computation). The quantity $f(|y|)$ will be referred to as the *integrand*. In practice, our strategy is to first compute $f(|y|)$ on a given set of values for $|y|$ and then do the last $|y|$-integral using the trapezoidal rule.

Due to current conservation, one is free to modify the QED kernel by subtracting a quantity that leads to a surface term vanishing in the infinite-volume limit [8]. Such a subtraction changes the shape of the 1-dimensional integrand but not $a_\mu^{\rm hlbl}$. In Ref. [6], we have proposed a family of subtracted kernels parametrized with a positive real number $\Lambda$. We can adjust $\Lambda$ in a way that $f(|y|)$ goes to zero fast enough in the large-$|y|$ region for a quicker convergence of the integrated $a_\mu^{\rm hlbl}$ without being too peaked at short-distances to avoid large discretization effects. Our default value for $\Lambda$ is 0.4.

The evaluation of the hadronic 4-point function $\tilde{\Pi}$ requires 5 different Wick-contraction topologies: the fully-connected, the (2+2), the (3+1), the (2+1+1) and the (1+1+1+1) (from left to right on Fig. 1). Note that the topologies involving self-contracted quark loops do not contribute in the limit of degenerate quark masses in $N_f = 3$. Based on this, we expect that the first two of the above topologies dominate. Henceforth, we will refer to the fully-connected and the (2+2) topologies as *leading topologies* whereas the remaining contributions are referred to as *sub-leading topologies*.

In each topology, there are a certain number of quark-contraction diagrams to be computed. As has already been noticed in our calculation with $\mathrm{SU}(3)_f$-symmetry ensembles [9], one can exploit translational-invariance of $\tilde{\Pi}$ to re-parametrize the integral representation of $a_\mu^{\rm hlbl}$ such that only a subset of computationally-cheap diagrams needs to be calculated upon a modification of the kernel function. See Ref. [5] for the exact expressions used for each topology.

## 3. Numerical setup

For our lattice simulation, we use fifteen $N_f = 2 + 1$ ensembles generated by the Coordinated Lattice Simulations (CLS) consortium [10] with five different lattice spacings and the lowest pion mass down to about 200 MeV (see Fig. 2).

Our propagator inversions are done with point-sources. To reduce the variance, we use the fact that, in infinite-volume, $f(|y|)$ is a scalar quantity under O(4)-transformations. Therefore all vectors $y$ which have the same norm should contribute equally to $f(|y|)$ in the limit of infinite statistics and in infinite-volume, and we can legitimately average the values for the integrand obtained with equivalent $y$-vectors under different choices of the origin.

A good determination of the (2+2)-disconnected contribution is crucial because it is known that it is of the same magnitude as the fully-connected contribution but of opposite sign [11]. On

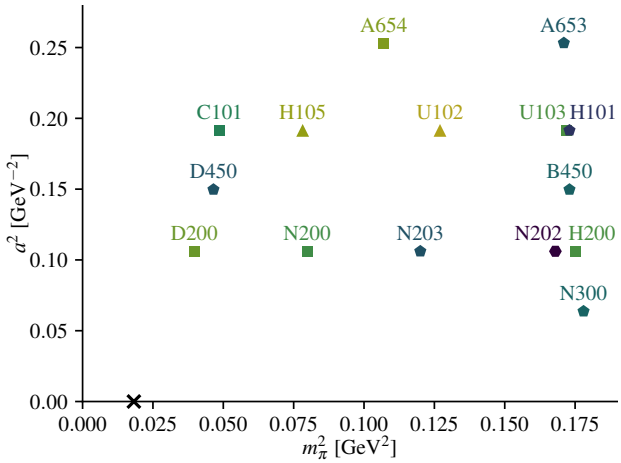


**Figure 2:** Overview of the ensembles used in this study. The symbols have $\lfloor m_\pi L \rfloor$ sides and darker colors correspond to large values of $m_\pi L$. The cross indicates the physical point.

top of the self-averaging strategy, we also rely on truncated solver techniques [12, 13] to reduce statistical fluctuations.

The subleading topologies, containing disconnected loops of type $\mathrm{Tr}[\gamma_\mu S(x,x)]$, where $S$ denotes the propagator, are expected to be small according to large-$N_c$ arguments and is partially supported by the findings of RBC/UKQCD collobaration [4]. In our work, we compute these loops based on the proposal of Ref. [14], which is a Wilson-fermion version of the One-End Trick commonly applied to the twisted-mass formulation, see e.g. Ref. [15]. Due to the electric charge factors, we always consider the difference between the light and strange disconnected loop in our computation when it comes to the subleading topologies. Finally, for the $(2+1+1)$, we precompute and store the lattice-wide object $\mathrm{Tr}[\gamma_\mu S(x,0)\gamma_\nu S(0,x)]$ for different choices of the origin in order to perform self-averaging more efficiently for noise reduction.

## 4. Results and analysis

In this talk, we only report the results for the purely light-quark part of the leading topologies (combining the fully-connected and the (2+2)-diagrams) and the (3+1) with light quark triangle, denoted by $(3+1)_{\mathrm{light}}$. The rest of the results can be found in the original paper [5].

### 4.1 The purely light-quark part of the leading topologies

On the left panel of Fig. 3, the fully-connected contributions to the partially integrated $a_\mu^{\mathrm{hlbl}}$ are shown for four ensembles at the same lattice spacing but different pion masses and $m_\pi L$. As the quality of the data in the large-$|y|$ region deteriorates, we apply a procedure to reconstruct the integrand in this region: we notice that our data can be well described by a simple exponential ansatz inspired by the $\pi^0$-pole contribution, which is the numerically dominant contribution to $a_\mu^{\mathrm{hlbl}}$. Considering theoretical arguments from Partially Quenched Chiral Perturbation Theory (PQChPT) [5] and our experience with the previous study at the $\mathrm{SU}(3)_f$-symmetry point [9], expectations are that the $\pi^0$-pole contributes in comparable size but opposite sign to the fully-connected and the (2+2). Therefore, we should expect a sizeable cancellation between the two.

As we can see from the right panel of Fig. 3, the combined fully-connected-(2+2) data points show a very flat pion-mass dependence — in contrast to the strong pion-mass dependence of the fully-connected contribution alone (left panel of Fig. 3) — which can in fact be well described by a simultaneous chiral, continuum and infinite-volume fit ansatz linear in $m_\pi^2$ and in $a^2$, with an exponentially suppressed term in $m_\pi L/2$.

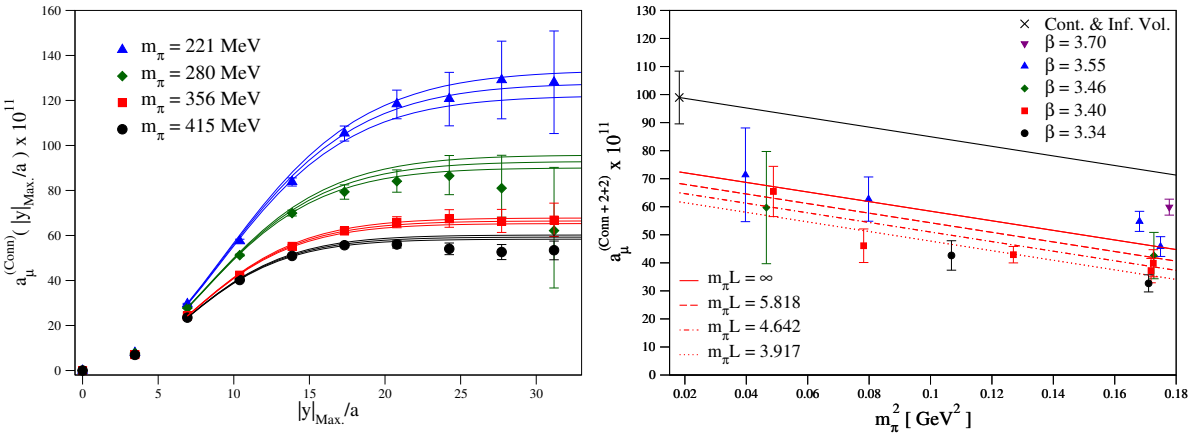


**Figure 3:** Left: Tail reconstruction for the partially integrated $a_\mu^{\rm hlbl}$ of the fully-connected contribution with $\beta = 3.4$ ($a^2 = 0.1915\,\text{GeV}^{-2}$) ensembles. Right: Global fit in $m_\pi^2$ and in $a^2$, with an exponentially suppressed term in $m_\pi L/2$. The red curves are for fixed $a$ with $\beta = 3.4$ at fixed $m_\pi L$ and the black one is the extrapolated result to the infinite-volume and continuum limit.

As for the systematic error of the extrapolation to the physical point, we identify several sources: the first is the lattice-spacing dependence of the ansatz that we use. On the left panel of Fig. 4, fit results are displayed with ansätze linear in $a$ or in $a^2$ performed at different cut datasets. The fits performed on the complete dataset give equally good $\chi^2$/d.o.f for both ansätze even though they differ by about $1\sigma$. Therefore, we decide to quote the result of the average of them for the purely light-quark leading-order contribution to $a_\mu^{\rm hlbl}$. A systematic error estimated from the root-mean-square deviation of the fits performed on different cut datasets as indicated on the left panel of Fig. 4 is assigned to our continuum extrapolation.

The second identified source of systematic error is due to the chiral extrapolation. In fact, a curvature term in $m_\pi^2$ is necessary if one extrapolates separately the fully-connected and the (2+2) to the physical pion mass. Several different curvature terms have been tried out and it is hard to tell if any one of them is superior to the others. Once combined to get the full leading-topology contribution, we see that all these different fits give very consistent results compared to our fit with the combined data, which allows for confidence in the validity of our procedure (right panel of Fig. 4). A reason why we are not really able to determine the curvature in $m_\pi^2$ is the larger error of our small-pion mass ensemble data.[1] From the left panel of Fig. 4, we see that when we exclude our heavier pion-mass ensembles, the errors of the fits grow significantly. To address the systematic error related to this, we perform another fit in replacing the linear $m_\pi^2$ dependence in the fit ansatz by $\log(m_\pi^2)$. This choice is inspired by the dominant light pseudoscalar meson prediction, namely the

[1] These ensembles are also, by far, our most computationally-expensive ensembles to generate data for.

$\pi^0$-pole (with a transition form factor (TFF) parametrized by the Vector-Meson-Dominance model) and the $\pi^\pm$-loop contributions. Among other fit ansatze that we have tried for the individual fits, such a term is the most divergent but still able to capture the chiral behavior for $m_\pi$ ranging from its physical value to 420 MeV, which corresponds to our heaviest pion mass used in this study. We quote half the difference between this alternative fit result and our original one for the systematic error for our chiral extrapolation.

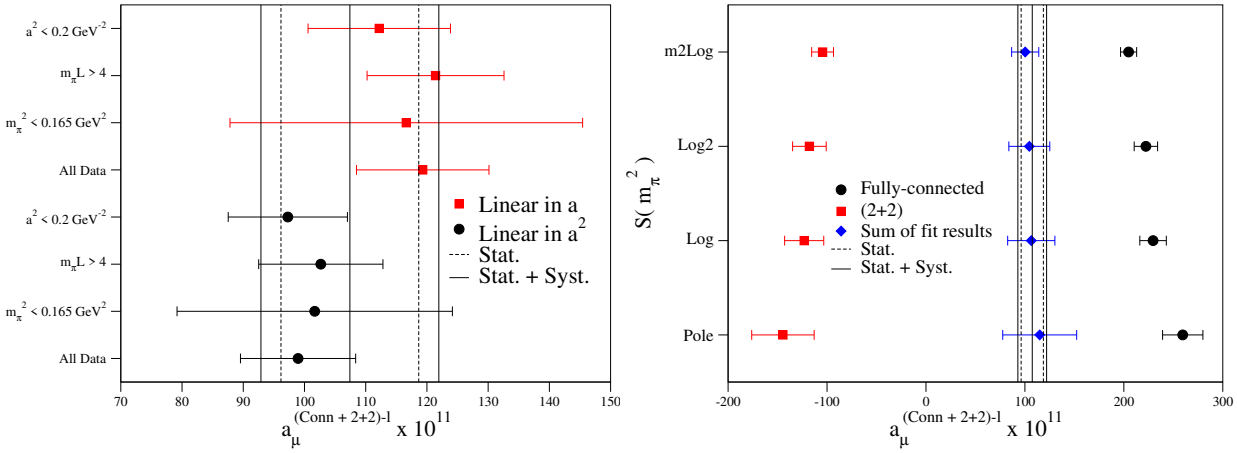


**Figure 4:** Left: $a$ v.s. in $a^2$, with different cuts in the data. Right: Combined v.s. summed separate fit results.

### 4.2 The $(3+1)_{\text{light}}$ topology

Among all the sub-leading topologies, we expect the (3+1) diagrams with a light quark "triangle", i.e. terms containing a factor of type $\text{Tr}[\gamma_\mu S(a,b)\gamma_\nu S(b,c)\gamma_\lambda S(c,a)]$, to be the dominant ones. From PQChPT, these diagrams receive a contribution proportional to the difference between the $\pi^\pm$- and the $K^\pm$-loops but none from the pseudoscalar meson-pole contribution at leading order. On all of our ensembles that are away from the $\text{SU}(3)_f$-symmetric point, the $(3+1)_{\text{light}}$ contribution turns out to be consistent with zero within error but the signal is quite rapidly lost when we go to larger $|y|$. Therefore, we come up with a treatment of the noisy tail of our data based on the prediction of the light-meson contribution. The procedure goes as follows, with a parameter $w_{\text{sys.}}$:

1. Compute the residual contribution from the pseudoscalar-meson loop $\delta a_\mu^{\text{PS}}$ from $|y| = |y|_{\text{cut}}$ to $|y| = \infty$.
2. Estimate the systematic error of the truncation as $w_{\text{sys.}} \times \delta a_\mu^{\text{PS}}$.
3. The central value is taken from the lattice data and the total error is the statistical and the systematic ones added in quadrature.
4. Choose $|y|_{\text{cut}}$ by minimizing the total error.

A typical outcome of this tail-truncation procedure is given in Fig. 5. In this example, the total error is minimized at around $|y| = 1.5$ fm and at this point, the total error is dominated by the statistical one.

The processed data points are shown on the left panel of Fig. 6, with $w_{\text{sys.}} = 100\%$. The data points are all consistent with zero but get noisier as the pion mass decreases. As there is no clear diverging trend in $m_\pi^2$, we chose the simplest ansatz $a_\mu^{(3+1)_{\text{light}}} = A(m_K^2 - m_\pi^2)$, which has an built-in constraint that this contribution vanishes at the $\text{SU}(3)_f$-symmetric point, without over-fitting the data with more complicated ansätze. To understand possible systematic errors related to our tail truncation procedure and our fitting, we repeat the same study with a couple of different values for $w_{\text{sys.}}$ ranging between 100% and 200% and perform the fit to different cut datasets (right panel of Fig. 6). We obtain very good consistency between all these different choices. For the final result, we quote the one from a conservative $w_{\text{sys.}} = 120\%$ with the coarsest lattice spacing left out.

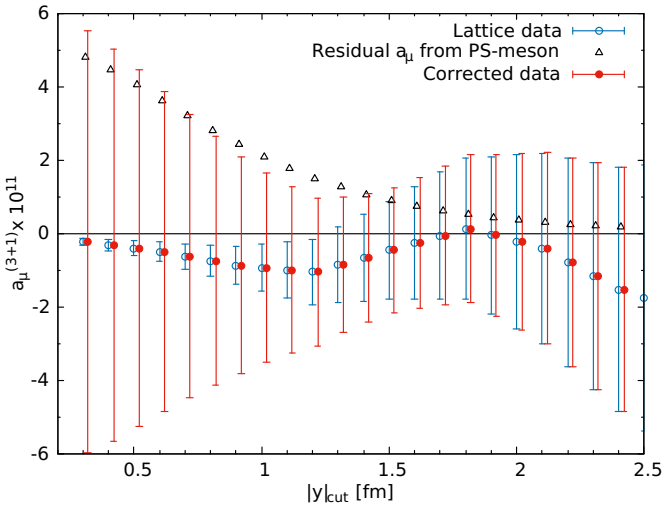


**Figure 5:** Example of the truncation procedure for the (3+1) with C101.

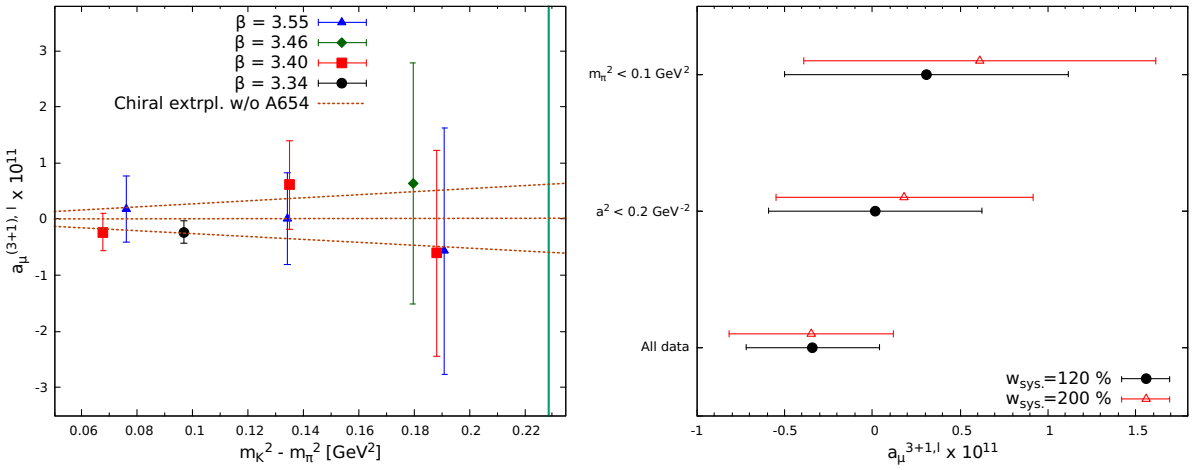


**Figure 6:** Left: Chiral extrapolation. Right: Consistency check.

## 5. Summary and outlook

In this talk, our lattice QCD determination of $a_\mu^{\rm hlbl}$ based on a position-space method obtained in Ref. [5] is presented. Accounting for all Wick-contraction topologies, we got a value of $a_\mu^{\rm hlbl} = 106.8(15.9)\times10^{-11}$, with a break-down in each topology given in Tab. 1. The precision requirement for resolving the present tension on $a_\mu$ between theory and experiment is achieved (see Fig. 7 for a comparison with other estimates). We provide evidence for the irrelevance of the contribution of the sub-leading topologies at the 10%-level precision for the total $a_\mu^{\rm hlbl}$ that we aim at. The ambiguity between the $\mathrm{O}(a)$ and $\mathrm{O}(a^2)$ discretization effects in the purely light-quark contribution from the leading topology makes us take a more conservative root-mean-squared approach for the systematic error estimation, which turns out to cover the spread of different cut datasets. In addition, we addressed the systematic error due to the chiral extrapolation, where our data are not accurate enough to allow for distinguishing the precise pion-mass dependence.

An improvement of this determination based on increasing the statistics on the lighter pion-mass ensembles would be computationally-daunting. Alternatively, one can also first subtract the most chirally dominant contributions from each data point at its respective pion mass, perform a global fit on the subtracted data, and finally add the subtracted contribution evaluated at the physical pion mass back to get the final estimate. Fig. 8 is an example of such a procedure, where the subtracted contribution is the $\pi^0$-pole contribution with TFF obtained from a dedicated lattice study [16]. In comparison to our original treatment, a flatter pion-mass dependence is apparent and the result obtained from this alternative approach is entirely compatible with our original result.

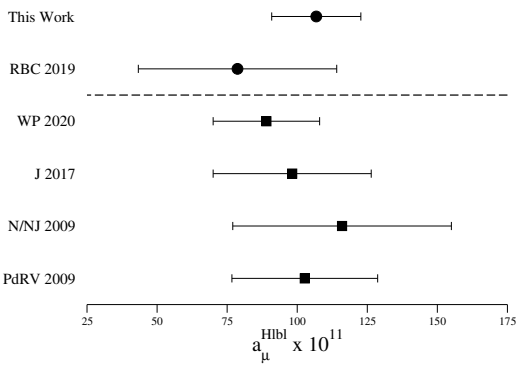


**Figure 7:** Comparison to the existing estimates. The circle ones are from lattice QCD and the square ones are phenomenological. See Ref. [5] for references.

## References

[1] B. Abi *et al.* [Muon g-2], Phys. Rev. Lett. **126** (2021) no.14, 141801.

[2] G. W. Bennett *et al.* [Muon g-2], Phys. Rev. D **73** (2006), 072003.

[3] T. Aoyama, N. Asmussen, M. Benayoun, J. Bijnens, T. Blum, M. Bruno, I. Caprini, C. M. Carloni Calame, M. Cè and G. Colangelo, *et al.* Phys. Rept. **887** (2020), 1-166.

| Contribution | Value$\times 10^{11}$ |
|---|---|
| Light-quark fully-conn. and (2 + 2) | $107.4(11.3)_{\text{stat.}}(9.2)_{\text{syst.}}(6.0)_{\text{chiral}}$ |
| Strange-quark fully-conn. and (2 + 2) | −0.6(2.0) |
| (3 + 1) | 0.0(0.6) |
| (2 + 1 + 1) | 0.0(0.3) |
| (1 + 1 + 1 + 1) | 0.0(0.1) |
| Total | 106.8(15.9) |

**Table 1:** A break-down table of the contribution for each Wick-contraction topology. The last error in the result of the light quark fully-conn. and (2+2) comes from the chiral extrapolation.

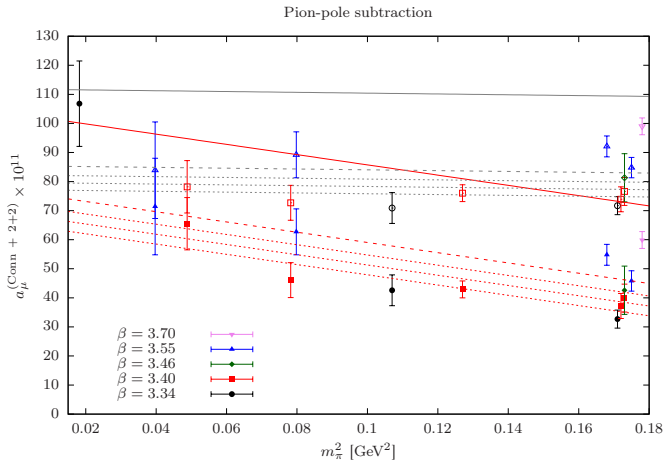


**Figure 8:** Red lines: original tail-reconstructed data. Black lines: with $\pi^0$-exchange computed on each ensemble individually subtracted and the continuum value added back at the physical pion mass. The dotted lines and dashed lines correspond to finite $m_\pi L$ (see Fig. 3) and infinite $m_\pi L$ at fixed $\beta = 3.4$ respectively and the plain lines are the results in the continuum and infinite-volume limit. The data point at the top left corner corresponds to our quoted final estimate for $a_\mu^{\text{hlbl}}$.

[4] T. Blum, N. Christ, M. Hayakawa, T. Izubuchi, L. Jin, C. Jung and C. Lehner, Phys. Rev. Lett. **124** (2020) no.13, 132002.

[5] E. H. Chao, R. J. Hudspith, A. Gérardin, J. R. Green, H. B. Meyer and K. Ottnad, Eur. Phys. J. C **81** (2021) no.7, 651

[6] N. Asmussen, E. H. Chao, A. Gérardin, J. R. Green, R. J. Hudspith, H. B. Meyer and A. Nyffeler, PoS **LATTICE2019** (2019), 195.

[7] N. Asmussen, J. Green, H. B. Meyer and A. Nyffeler, PoS **LATTICE2016** (2016), 164.

[8] T. Blum, N. Christ, M. Hayakawa, T. Izubuchi, L. Jin, C. Jung and C. Lehner, Phys. Rev. D **96** (2017) no.3, 034515.

[9] E. H. Chao, A. Gérardin, J. R. Green, R. J. Hudspith and H. B. Meyer, Eur. Phys. J. C **80** (2020) no.9, 869.

[10] M. Bruno, D. Djukanovic, G. P. Engel, A. Francis, G. Herdoiza, H. Horch, P. Korcyl, T. Korzec, M. Papinutto and S. Schaefer, *et al.* JHEP **02** (2015), 043.

[11] J. Bijnens and J. Relefors, JHEP **09** (2016), 113

[12] G. S. Bali, S. Collins and A. Schafer, Comput. Phys. Commun. **181** (2010), 1570-1583.

[13] T. Blum, T. Izubuchi and E. Shintani, Phys. Rev. D **88** (2013) no.9, 094503.

[14] L. Giusti, T. Harris, A. Nada and S. Schaefer, Eur. Phys. J. C **79** (2019) no.7, 586.

[15] K. Jansen *et al.* [ETM], Eur. Phys. J. C **58** (2008), 261-269.

[16] A. Gérardin, H. B. Meyer and A. Nyffeler, Phys. Rev. D **94** (2016) no.7, 074507